Environment International 186 (2024) 108569

Contents lists available at ScienceDirect

Environment International

journal homepage: www.elsevier.com/locate/envint

Full length article

Exposure to environmental toxicants is associated with gut microbiome dysbiosis, insulin resistance and obesity

Partho Sen [a,b], Yong Fan [c], Jennifer J. Schlezinger [d], Stanislav D. Ehrlich [e], Thomas F. Webster [d], Tuulia Hyötyläinen [f,*], Oluf Pedersen [c,g,*], Matej Orešič [a,b,*]

[a] Turku Bioscience Centre, University of Turku and Åbo Akademi University, 20520, Turku, Finland
[b] School of Medical Sciences, Faculty of Medicine and Health, Örebro University, 702 81, Örebro, Sweden
[c] Novo Nordisk Foundation Center for Basic Metabolic Research, Faculty of Health and Medical Sciences, University of Copenhagen, 2200, Copenhagen, Denmark
[d] Department of Environmental Health, Boston University School of Public Health, Boston, MA, USA
[e] Department of Clinical and Movement Neurosciences, UCL Queen Square Institute of Neurology, London WC1N 3RX, UK
[f] MTM Research Centre, School of Science and Technology, Örebro University, 702 81, Örebro, Sweden
[g] Center for Clinical Metabolic Research, Herlev-Gentofte University Hospital, Copenhagen, Denmark

ARTICLE INFO

Handling Editor: Olga Kalantzi

Keywords:
PFAS
Gut microbiome
Obesity
Insulin resistance
Serum bile acids

ABSTRACT

Environmental toxicants (ETs) are associated with adverse health outcomes. Here we hypothesized that exposures to ETs are linked with obesity and insulin resistance partly through a dysbiotic gut microbiota and changes in the serum levels of secondary bile acids (BAs). Serum BAs, per- and polyfluoroalkyl substances (PFAS) and additional twenty-seven ETs were measured by mass spectrometry in 264 Danes (121 men and 143 women, aged 56.6 ± 7.3 years, BMI 29.7 ± 6.0 kg/m^2) using a combination of targeted and suspect screening approaches. Bacterial species were identified based on whole-genome shotgun sequencing (WGS) of DNA extracted from stool samples. Personalized genome-scale metabolic models (GEMs) of gut microbial communities were developed to elucidate regulation of BA pathways. Subsequently, we compared findings from the human study with metabolic implications of exposure to perfluorooctanoic acid (PFOA) in PPARα-humanized mice. Serum levels of twelve ETs were associated with obesity and insulin resistance. High chemical exposure was associated with increased abundance of several bacterial species *(spp.)* of genus *(Anaerotruncus, Alistipes, Bacteroides, Bifidobacterium, Clostridium, Dorea, Eubacterium, Escherichia, Prevotella, Ruminococcus, Roseburia, Subdoligranulum, and Veillonella)*, particularly in men. Conversely, females in the higher exposure group, showed a decrease abundance of

Abbreviations: AGORA, assembly of gut organisms through reconstruction and analysis; ADE, Average direct effect; ACME, Average causal mediation effect; AUC, area under the receiver operating characteristic curve; BAs, bile acids; BMI, Body Mass Index; BSH, bile salt hydrolase; CA, cholic acid; CDCA, chenodeoxycholic acid; CYP450, cytochrome P450; CYP34A, Cytochrome P450 3A4; EMP, estimated metabolic potential; FXR, farnesoid X receptor; GCA, glycocholic acid; GCDCA, glycochenodeoxycholic acid; GCDCA-S, glycochenodeoxycholate-3-sulfate; GDCA, glycodeoxycholic acid; GEMs, genome-scale metabolic models; GSMM, genome-scale metabolic modeling; HCA, hyocholic acid; HOMA-IR, homeostatic model assessment of insulin resistance; hPPARα, Humanized PPARα mouse model; LR, logistic ridge regression; MCA, muricholic acids; MetaHIT, metagenomics in human intestinal tract; MS, mass spectrometry; SCFAs, short-chain fatty acids; TCA, taurocholic acid; TDCA, taurodeoxycholic acid; THCA, taurohyocholic acid; TαMCA, tauro-α-muricholic acid; UDCA, ursodeoxycholic acid, DCA, deoxycholic acid; UPLC-QqQMS, ultra-performance liquid chromatography-tandem mass-spectrometry; VH, vehicle; VMH, virtual metabolic human database; 1OH-n:2 FTSAs, 1 OH-substituted n:2 fluorotelomer sulfonic acids; BPA sulfate, Bisphenol A sulfate; dPAs, double bond-perfluoroalkyl alcohols; dPFAm, double bond perfluoroalkyl amines; dPFAmCACEs, double bond perfluoroalkyl amine carboxylic acids/carboxyl esters; dPFLSA, double bond perfluoroalkyl (linear) sulfonic aicds; HPFLSA, H-substituted perfluoroalkyl sulfonic acids; K/d-O/CO-PFLSA, Ketone-/double bond-ether-/cyclic-ether- perfluoroalkyl (linear) sulfonic acids; mHPFLCA, multiple H-substituted perfluoroalkyl carboxylic acids; mHPFLCA, multiple H-substituted perfluoroalkyl (linear) carboxylic acids; mHPFSO4_ii, multiple H-substituted perfluoroalkyl sulfates_ii; mOPFLCA, multiple ether-substituted perfluoroalkyl caborxylic acids; n:1 FTSAs, n:1 fluorotelomer sulfonic acids; n:2 FTOHs, n:2 fluorotelomer alcohols; n:2 FTSAs, n:2 fluorotelomer sulfonic acids; n:2 FTSAs, n:2 fluorotelomer sulfonyl propanoic acids; n:2 FTSO2PAs, 1 OH-substituted n:2 fluorotelomer sulfonic acids*; n:2 FTSPrAs, n:2 fluorotelomer thio proponic acids; OPFLCA_i, ether-substituted perfluoroalkyl caborxylic acids_i; PFAABs, perfluoroalkylamido betaine-related; PFAmCACEs, perfluoroalkyl amine carboxylic acids/carboxyl esters; PFAmCEs_i, perfluoroalkyl amine carboxyl esters_i; PFDA, Perfluorodecanoic acid; PFHxS, perfluorohexanesulfonic acid; PFNA, perfluorononanoic acid; PFOA, perfluorooctanoic acid; PFOS, perfluorooctanesulfonic acid; qaPFSMb, N-methyl perfluoroalkanesulfonamido quaternary ammonium; qaPFSMe, perfluoroalkanesulfonamido quaternary ammonium diol A; qaPFSMf, perfluoroalkanesulfonamido quaternary ammonium diol B.

* Corresponding authors at: School of Medical Sciences, Örebro University, Örebro, Sweden.
E-mail addresses: tuulia.hyotylainen@oru.se (T. Hyötyläinen), oluf@sund.ku.dk (O. Pedersen), matej.oresic@oru.se (M. Orešič).

https://doi.org/10.1016/j.envint.2024.108569
Received 13 November 2023; Received in revised form 5 March 2024; Accepted 6 March 2024
Available online 20 March 2024

Prevotella copri. High concentrations of ETs were correlated with increased levels of secondary BAs including lithocholic acid (LCA), and decreased levels of ursodeoxycholic acid (UDCA). *In silico* causal inference analyses suggested that microbiome-derived secondary BAs may act as mediators between ETs and obesity or insulin resistance. Furthermore, these findings were substantiated by the outcome of the murine exposure study. Our combined epidemiological and mechanistic studies suggest that multiple ETs may play a role in the etiology of obesity and insulin resistance. These effects may arise from disruptions in the microbial biosynthesis of secondary BAs.

1. Introduction

Human epidemiological studies show that large number of environmental toxicants (ETs) such as bisphenols, phthalates, pesticides, persistent organic pollutants (POPs), heavy metals and per- and polyfluoroalkyl substances (PFAS) are detected in humans and they have endocrine-disrupting effects, including adverse metabolic impacts (Oresic et al., 2020). Indeed, ETs are associated with a variety of adverse health outcomes including reproductive and developmental defects, immune and metabolic dysfunction, as well as cardiometabolic disease, as shown in both human studies as well as using *in vivo* and *in vitro* toxicological models (Ammitzbøll et al., 2019; Armstrong and Guo, 2019; Cardenas et al., 2017; Christensen et al., 2019; Geng et al., 2019; Hyotylainen et al., 2024; Louisse et al., 2023; McGlinchey et al., 2019; Oresic et al., 2020; Qi et al., 2020; Sinioja et al., 2022). In addition to direct effects of ET exposure, several ETs have shown to have an impact on gut microbiota (Jin et al., 2017). One of the major routes of exposures is *via* contaminated food and water, making the gastrointestinal track the first contact point of exposure. ETs can modify the gut microbiota, and consequently, impact the microbiota produced metabolites and host metabolism.

One ET group of particular interest are PFAS, a group of synthetically produced chemicals that are classified as endocrine-disrupting chemicals. They are widely used in products such as nonstick cookware, water-repellent clothing, stain resistant fabrics and carpets, some cosmetics, some firefighting foams, and products that resist grease, water and oil. Due to their widespread use, these compounds can be detected in nearly entire human population, PFAS being one of the most abundant ETs detected in humans. The general population is exposed to PFAS mainly through diet and drinking water, and these persistent compounds gradually accumulate in the liver (half-life of 2–5 years) (Behr et al., 2020b). PFAS exposure has been associated with a variety of health effects (Fenton et al., 2021). Particularly, PFAS have been suggested to contribute to the pathogenesis of metabolic dysfunction-associated steatotic liver disease (MASLD) in a sex-dependent manner (Deierlein et al., 2017; Rantakokko et al., 2015; Sen et al., 2022). PFAS are known to be enriched in the liver (Nielsen et al., 2024), where they can also interfere with the glucose and lipid metabolism (Deierlein et al., 2017). Structurally, PFAS have high similarity to fatty acids (FAs) and they have been shown to disrupt hepatic lipid metabolism by interacting with multiple nuclear receptors, including peroxisome proliferator-activated receptors (PPARs) (Behr et al., 2020a; Hyotylainen et al., 2024). They also interfere with the biosynthesis of the bile acids (BAs), their enterohepatic circulation, and gut microbial modification of BAs (Hyotylainen et al., 2024; Salihović et al., 2019; Sen et al., 2021; Zhao et al., 2015).

BAs have major roles not only in digestion and absorption of fats and fat-soluble vitamins in the small intestine, but also in regulation of lipid and glucose metabolism (Yu et al., 2023). BAs are synthesized in the liver from cholesterol to produce cholic acid (CA) and chenodeoxycholic acid (CDCA). BAs are conjugated with (mainly) glycine or taurine and released into the bile. When released to gastrointestinal tract, primary BAs undergo biotransformation (deconjugation of the glycine or taurine, dehydroxylation, dehydrogenation, and epimerization) by the intestinal microbes to form secondary BAs (Guzior and Quinn, 2021; Lamichhane et al., 2022; Petersen et al., 2021; Wahlstrom et al., 2016). PFAS can interfere with the biosynthesis of BAs by suppressing the expression of 7-alpha-hydroxylase (CYP7A1) which catalyzes the first and rate-limiting step in the formation of BAs from cholesterol (Beggs et al., 2016; Behr et al., 2020b). In turn, decreased CYP7A1 might increase re-uptake of BAs by triggering negative feedback loops *via* the farnesoid X receptor (FXR), subsequently decreasing the *de novo* synthesis of primary BAs from cholesterol (Pandak and Kakiyama, 2019). Recently, European Food Safety Authority (EFSA) published a scientific opinion suggesting that the total serum cholesterol levels are positively associated with the levels of two major PFAS, perfluorooctane sulfonate (PFOS) and perfluorooctanoic acid (PFOA) (Andersen et al., 2021). PFOS and PFOA might share common membrane transporters and enterohepatic circulatory pathways with BAs (Behr et al., 2020b; Hyotylainen et al., 2024; Salihovic et al., 2020).

The impacts of chemical exposure on gut microbiome and BA pathways in humans are still sparsely explored (Chiu et al., 2020; Claus et al., 2016). The host-microbiota metabolic homeostasis can be modified by exposure to ETs, as shown in the murine studies (Lai et al., 2018; Zhang et al., 2020). For example, exposure to dioxins has shown to disrupt the gut microbiome and induced liver toxicity in mice by increasing total BAs and short-chain fatty acids (SCFAs), whilst decreasing FXR signaling in liver (Wang et al., 2019; Zhang et al., 2017).

Here we hypothesized that exposure to ETs is associated with altered BA metabolism, gut microbiome dysbiosis, insulin resistance and obesity. We investigated the impact of exposure to ETs, with specific focus on PFAS and other organofluorines, in the MetaHIT (Metagenomics of the Human Intestinal Tract) cohort. The MetaHIT cohort studies have shown that dysbiosis of the gut microbiome is associated with obesity and insulin resistance (Le Chatelier et al., 2013; Pedersen et al., 2016; Petersen et al., 2021) and that serum levels of specific C-6-hydroxylated bile acids are associated inversely with measures of adiposity (Petersen et al., 2021). These C-6-hydroxylated BAs were linked with the gut microbial community composed of Clostridia species (*spp.*) (Petersen et al., 2021).

We analyzed ETs using both target and suspect screening methods and BAs in fasting serum samples from 264 Danish adults from the MetaHIT cohort and integrated these data with gut microbiota data derived from whole-genome shotgun (WGS) sequencing of DNA extracted from purified stool samples. The main emphasis was on PFAS and other organofluorine compounds due to their high detection frequency and their suspected effects both in human gut microbiota and host metabolism.

2. Materials and methods

2.1. Study subjects

ETs and BAs were measured in fasting serum samples obtained from 264 nondiabetic Danes, 143 women and 121 men. The study participants were recruited from the Danish Inter99 study (Le Chatelier et al., 2013; Pedersen et al., 2016; Petersen et al., 2021) (Table 1). None of the volunteers have undergone bariatric surgery or had taken antibiotics two months prior to their inclusion in the study. The median age of the study population was 56.6 ± 7.3 years, mean Body Mass Index (BMI) was 29.7 ± 6.0 kg/m^2, and mean HOMA-IR was 2.0 ± 1.4. Thirty-four study participants were taking statins at the time of study. Obesity in

Table 1
Demographic and clinical characteristics of the study subjects. Blood for analyses of biochemical values were taken in the morning in the fasting state. Values are presented as (mean ± standard deviation, SD). 'n' denotes number of subjects.

Clinical features	Subjects (n)	Values (mean ± SD)
Age (years)	264	56.6 ± 7.25
Sex		
males	121	
females	143	
BMI (kg/m^2)		29.68 ± 5.98
High (>29.7 kg/m^2)	168	33.57 ± 3.58
Low	96	22.86 ± 1.71
HOMA-IR		2.0 ± 1.42
High (>2.5)	78	3.70 ± 1.39
Low	184	1.27 ± 0.57
Waist circumference (cm)		100.02 ± 16.29
HDL (plasma, mmol/L)		1.54 ± 0.53
LDL (plasma, mmol/L)		3.35 ± 0.84
Obesity		
Obese	155	
Non-Obese	109	
Current smoker		
Yes	39	
No	225	
Previous smoker		
Yes	117	
No	147	
Medication (statins and/or biguanides)		
Yes	36	
No	228	

this study was defined as BMI > 27 kg/m^2. Details of clinical and biochemical phenotyping have been previously reported (Le Chatelier et al., 2013; Pedersen et al., 2016; Petersen et al., 2021).

2.2. Ethics statement – Clinical study

The MetaHIT study was approved by the local Ethical Committees of the Capital Region of Denmark (HC-2008-017) and was in accordance with the principals of the Declaration of Helsinki. All individuals gave written informed consent before participation in the study.

2.3. Ethics statement – Murine study

All animal studies were approved by the Institutional Animal Care and Use Committee at Boston University and performed in an American Association for the Accreditation of Laboratory Animal Care accredited facility (Animal Welfare Assurance Number: A3316-01).

2.4. Murine exposure study

The exposure study protocol using a humanized PPARα (hPPARα) mouse model was reported previously (Schlezinger et al., 2021; Schlezinger et al., 2020). A summary is provided in the **Supplementary Information**.

2.5. Analysis of environmental toxicants and bile acids in serum

Serum levels of ETs and BAs were assessed by ultra-performance liquid chromatography coupled to a quadrupole time-of flight mass spectrometry (UHPLC-QTOFMS), using a sample preparation procedure as previously described (Sen et al., 2022). The determination of ETs included target analysis of specific compounds and suspect screening approach based on Norman network database (https://www.norman-network.com/nds/SLE/). Method details are provided in the **Supplementary Information**.

2.6. Gut microbiome profiling

Anonymized raw metagenomic sequencing data of 264 subjects participated in this study was retrieved from European Nucleotide Achieve (ENA) (https://www.ebi.ac.uk/ena/browser/view/PRJEB4336)(Le Chatelier et al., 2013; Pedersen et al., 2016; Petersen et al., 2021). Host genome–contaminated reads and low-quality reads were removed from the sequencing data using KneadData v0.4. Taxonomic profiles were determined using MetaPhlAn2 (Segata et al., 2012; Truong et al., 2015) using default parameters. A detailed protocol for stool sampling, DNA purification, library preparation, WGS, and quality control of sequencing reads have been previously reported (Le Chatelier et al., 2013; Pedersen et al., 2016; Petersen et al., 2021). The raw data were processed, and taxonomic profiling and compositional analysis were performed.

2.6.1. Characterization of gut bacterial genetics

Prior to classification of bacterial structural variations (SVs) into deletion SVs (dSVs) and variable SVs (vSVs), a bioinformatics pipeline using an iterative coverage-based read assignment (ICRA) was carried out to accurately reassign ambiguous reads to the most likely reference bacterial genomes (Wang et al., 2021; Zeevi et al., 2019). The reference bacterial genomes provided in the proGenomes database (http://progenomes1.embl.de/) were then concatenated and segmented into 1-kbp bins, which was used for detection of highly variable segments. SGV-Finder pipeline was implemented to profile genomic bins that were either present in < 25 % of the studied individuals (called vSVs), or present in 25–75 % of the studied subjects, in which the absence or presence were kept (called dSVs) (Zeevi et al., 2019). Genomic bins presenting in > 75 % of the cohort were not considered in the analysis.

2.7. Statistical analysis

R statistical programming language (v.3.6.0) (R Development Core Team, 2018) was used for data analysis. The *'Heatmap.2'*, *'boxplot'*, *'beanplot'*, *'gplot'*, and *'ggplot2'* libraries / packages were used for data visualization. Prior to analyses, ETs, BAs, and relative taxonomic abundances of the microbes were $\log_2$ transformed with a plus one pseudocount.

2.7.1. Univariate analysis

Mann-Whitney U test was used to assess differences in the concentration of the ETs. The p-values were adjusted for multiple testing at False Discovery Rate, FDR ($p < 0.05$). The effect-size using mean differences was determined by Cohen's d using *'effsize'* (v0.8.1) package in R.

2.7.2. Bivariate correlation analysis

Likewise, *'RcmdrMisc'* package was used to estimate Spearman's correlation between the total ETs. The p-values were adjusted for multiple testing at (FDR, $p < 0.05$). Results were plotted using *heatmap.2* function of *'gplots'* package (v.3.0.4).

2.7.3. Factor analysis

ETs, BAs and microbial abundance datasets were centered to zero mean and unit variance (autoscaled). The relative contribution of a clinical/demographic factor towards the total variance in these datasets were estimated by fitting a linear regression model, where the ETs or BAs or microbial abundance were regressed to a clinical/demographic factor of interest, and median marginal coefficient of determination (R^2) were estimated. Factor analysis was performed using the *'Scater'* package deployed in R. The results were further confirmed by Permutational Multivariate Analysis of Variance (PREMANOVA) (t = 999) using Bray-Curtis dissimilarity index.

2.7.4. Model-based clustering

Thirty-five ETs were classified into three distinct environmental toxicant clusters (ETCs) using the '*mclust*' R package (v.5.4.6). *Mclust* is a model-based 'unsupervised' clustering method which explore and analyze complex data sets by grouping similar observations into clusters based on their statistical properties. The clustering process in *Mclust* involves fitting various Gaussian mixture models to the data, and subsequently choosing the model that most accurately matches the data. The method uses a maximum likelihood approach to estimate the model parameters, including the number of clusters, the mean and covariance matrix of each cluster, and the mixing proportions that determine the probability of each observation belonging to each cluster. It can automatically determine the optimal number of clusters in the data. Herein, the model performances were evaluated by the Bayesian Information Criterion (BIC). The models with the highest BICs were chosen. Mean cluster profile of each ETC was divided into quartiles (Q1-Q4); where Q1, Q2-3, Q4 denote low, intermediate, and high chemical exposure levels, respectively.

2.7.5. Gradient-boosted decision trees (GBDT) and feature attribution analysis (SHAP)

To understand the association of the ETs with the BMI, HOMA-IR and obesity, we developed Gradient-boosted decision trees (GBDT) models. These models were adjusted for the confounding effects of sex and age at visit of the subjects, as determined by the factor analysis. A detail on GBDT and SHAP analysis are described in the **Supplementary Information**.

2.7.6. Linear discriminant analysis

Linear discriminant analysis Effect Size (LEfSe) (Segata et al., 2011) was performed to determine whether the features (BAs and microbes) were differentially regulated between two classes/groups (obese *vs.* non-obese, and high *vs.* low HOMA-IR in both males and females). Linear discriminant analysis (LDA) scores or effect size of a feature that passed the statistical significance (Mann-Whitney U test, p-values adjusted for FDR < 0.05) was selected.

2.7.7. Estimation of alpha- and beta-diversity of the gut microbiome

Alpha-diversity (Shannon-Weiner index), richness and evenness (pielou) of the gut microbiome in the exposure groups (high Q1-Q4 low) within the ETCs were estimated by using '*vegan*' package in R. A decrease in the alpha-diversity was determined by (Kruskal–Wallis one-way analysis of variance, p adjusted for FDR < 0.05). Beta-diversity the gut microbiome among the exposure groups (Q1 and Q4) in the ETCs were estimated by principal coordinate analysis (PCoA) using Bray-Curtis dissimilarity index.

2.7.8. Deconfounding and mediation analysis

Deconfounding analysis was performed using '*metadeconfoundR*' R package (v0.2.8) (Fromentin et al., 2022). Mediation analysis was performed using '*mediation*' R package (v4.5.0) in R. Details of the analyses are described in the **Supplementary Information**.

2.8. Genome-scale community modeling of gut microbiota

We used genome-scale metabolic modeling (GSMM) applying Assembly of Gut Organisms through Reconstruction and Analysis (AGORA) (Heinken et al., 2023; Magnusdottir et al., 2017) to model BA biotransformation exhibited by the gut microbiome when exposed to ETs. Recently, GSMM has been applied to elucidate the role of gut microbiota in BA biotransformation in humans (Heinken et al., 2019). To reduce the complexity of GSMM (community modeling), we included genome-scale metabolic models (GEMs) of thirty-one out of sixty-seven abundant gut microbial species, including several strains detected in the metagenomic dataset that were linked with at least one ETC and had BA biosynthetic pathways. All the microbial-GEMs were retrieved from the '*AGORA_BA*' compendium (v1.03) (Heinken et al., 2019; Magnusdottir et al., 2017) – Virtual Metabolic Human Database (VMH) (Noronha et al., 2019), and assessed for further analysis. Details of GSMM and the development of personalized community models are given in **Supplementary Information**.

3. Results

3.1. Serum concentrations of ETs associate with obesity and insulin resistance

ETs were measured in fasting serum samples in 264 individuals who participated in the MetaHIT study (Pedersen et al., 2016; Petersen et al., 2021) (Table 1). A total of thirty-five unique chemical compounds including eight PFAS (target analyses) and twenty-seven additional ETs (based on suspect screening fluorine containing organic substances) were determined (**Fig. S1**, **Table S1**). Serum concentration of total PFAS were 15 % higher (Cohen's d = 0.42 at 95 % confidence interval [CI: 0.17——0.60]; Mann-Whitney U test at p = 0.0004) in males as compared to females (Fig. 1**A**, **Table S2**). Factor analysis showed that various clinical and demographic factors were associated with ETs. Specifically, chemical exposure (ETs) was positively associated with age and sex of the subjects (percentage of explained variance, EV > 1 %) (Fig. 1**B**), whilst the use of medication had a minor or no effect on the ETs. In addition, results of deconfounding analysis showed that association between ETs and outcomes were confounded by age of the individuals, and age was positively correlated with several ETs (**Fig. S2**).

In order to study the associations between ETs and metabolic measures such as body mass index (BMI), homeostatic model assessment for insulin resistance (HOMA-IR), and obesity (dichotomized at mean BMI = 29.7 kg/m^2), we developed gradient-boosted decision tree (GBDT)(Ke et al., 2017) models adjusted for the confounding effects of age and sex (**Materials and methods**). SHapley Additive exPlanations (SHAP) (Lundberg et al., 2018) values derived from these models suggested that serum concentration of several ETs (dPAs n = 0, PFHxS, dPFLSA n = 5, PFAAb n = 7, BPA sulphate, PFDA, dPFAMs, n = 2 FTOHs n = 2, PFOS_branched, etc.) were positively associated with BMI (Fig. 1**C**). In addition, some of these ETs were positively associated with HOMA-IR and obesity (Fig. 1**D**, **Fig. S3**). Serum concentrations of dPAs n = 0 and FTOHs n = 2 were higher (log of linear discriminant analysis, LDA score $> +2.5$) in obese females with high HOMA-IR (>2.5) as compared to non-obese females (Fig. 1**E**). Collectively, serum concentration of twelve ETs were associated with BMI, HOMA-IR and obesity (Fig. 1**F**, **Fig. S4**).

3.2. Fasting serum concentrations of clusters of ETs associate directly with fasting serum levels of secondary BAs

Serum concentrations of ETs exhibited strong correlations among themselves (**Fig. S1**). A finite Gaussian mixture modeling, an 'unsupervised' learning method that does not rely on any predefined categories to group the observations, was used to classify ETs. Thirty-five ETs were divided into three distinct environmental toxicant clusters (ETC1–3).

ETC1 mainly comprised of PFAS, whilst ETC2 and ETC3 mainly included sulphonated and fluorinated compounds, respectively (**Fig. S5**). Mean cluster profiles of ETC were regressed on serum BA concentrations adjusted for the confounding effects of age and sex, and SHAP values were estimated. ETC1 and 3 showed strong positive association with lithocholic acid (LCA) (Fig. 2**A, 2C**), and to a lesser extent with hyocholic acid (HCA). All three ETCs positively associated with 6- and 7-ketolithocholic acids (Fig. 2**A-C**). ETC2 and 3 were positively associated with glycochenodeoxycholate-3-sulfate (Glyco-CDCA-3-O sulphate/GCDCA-S), and ETC3 with tauro-α-muricholic acid (TαMCA). In contrast, ETC1–3 showed strong inverse associations with ursodeoxycholic acid (UDCA), CDCA, deoxycholic acid (DCA) and/or their conjugates (Fig. 2**A-C**). These results suggest that high chemical exposure

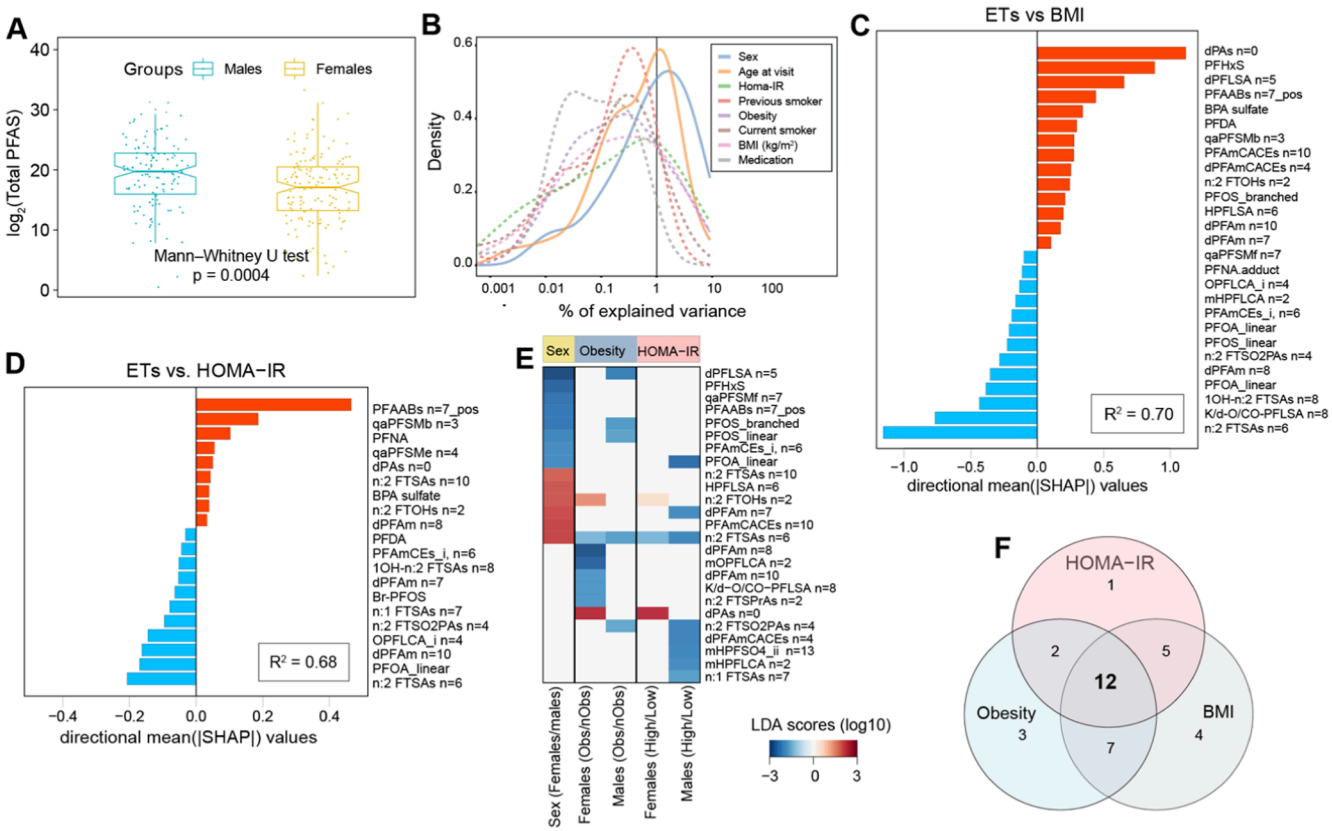

Fig. 1. Environmental toxicants that are associated with obesity and insulin resistance. (A) A boxplot showing $\log_2$ intensities of total PFAS in females (n = 143) and males (n = 121) (Mann–Whitney U test, $p < 0.05$ adjusted for FDR). Subjects are denoted by dots. **(B)** A density plot showing sample-wide distribution of (percentage of explained variances, EV) of various clinical and demographic factors associated with serum concentrations of environmental toxicants (ETs). **(C, D)** The directional mean |SHAP| values of ETs associated with BMI and HOMA-IR, estimated by the gradient-boosted decision tree (GBDT)–regression models adjusted for the confounding effects of age and sex of the subjects. The model performances are given as a mean R-squared (coefficient of determination). '+ve' and '-ve' SHAP values are illustrated by light red and blue colors respectively. **(E)** Heatmap showing the differences in the intensities of ETs, represented by log (LDA scores / effect size) in the obese (Obs) *vs.* non-obese (nObs) (dichotomized at 27 kg/m^2), and high *vs.* low (HOMA-IR, dichotomized at 2.5) females and males. '+ve' and '-ve' LDA scores are denoted by red and blue colors respectively. LDA scores that pass the statistical significance (Wilcoxon signed-rank test, $p < 0.05$) are shown. **(F)** Venn diagram showing ETs that are directly associated with the obesity, HOMA-IR and BMI. (For interpretation of the references to colour in this figure legend, the reader is referred to the web version of this article.)

might elevate serum levels of LCAs, 7-ketolithocholic acid (an intermediate in the conversion of CDCA to UDCA) and HCA, whilst lowering the levels of UDCA and CDCA (Fig. 2**A-C**).

The serum level of LCA was significantly higher (with a log LDA > +2.5) in obese males with high HOMA-IR compared to their non-obese male counterparts while no such differences were observed in females (Fig. 2**D**). In addition, all males had higher levels of LCA, HCA, and GCA in their serum than females (with statistical significance based on Mann-Whitney U test, p-values adjusted for FDR < 0.05), Fig. 2**E**). Interestingly, the obese females with or without high HOMA-IR had elevated levels of UDCA, GUDCA and DCA, whilst reduced serum levels of 7-ketolithocholic acid (Fig. 2**D**).

3.3. Dysbiosis of gut microbiota associates with exposure to ETs

As expected, compositional analysis of gut microbiota showed that Bacteroidetes and Firmicutes were the two most dominant microbial phyla (Fig. 3**A-C**, **Fig. S7**). High chemical exposure (Q4, n = 66) to ETC3 compounds showed a disproportionately higher abundance of Firmicutes over Bacteroidetes phyla (Fig. 3**C**).

In addition, markedly lower values (Kruskal-Wallis test, $p < 0.05$) of alpha-diversity (Shannon-Weiner Index), richness and evenness (pielou) of gut microbiota were observed in the high Q4 ET exposure group (Fig. 3**D-E**). Beta-diversity (Bray-Curtis dissimilarity index) of high *vs.* low exposure ET groups did not show a distinct separation. However, the results of principal coordinate analysis (PCoA) showed that within the ETC3 cluster, there was an observed differentiation between the microbiomes of at least twenty individuals in the high exposure group (Q4) as compared to the low exposure group (Q1), as illustrated in (Fig. 3**F**) (highlighted with green dots). No such changes were observed in the ETC1 or ETC2 clusters.

3.4. Gut bacteria associate with ETs in a sexually dimorphic manner

Our study demonstrates that exposure to ETs can disrupt the balance of gut microbiota, potentially leading to increased risk of obesity and insulin resistance (Fig. 3). To investigate the non-linear relationship between ETs and gut bacteria, we developed GBDT models separately for males and females, and estimated the directional SHAP values (**Materials and methods**). Interestingly, certain bacterial species showed sex-specific associations (non-zero SHAP values) with ETs.

In females, abundance of *Alistipes onderdonkii*, *Alistipes shahii, Ruminococcaceae bacterium D16, Ruminococcus albus, Ruminococcus flavefaciens, Bacteroides thetaiotaomicron, Bacteroides dorei, Bacteroides ovatus, Veillonella* spp., *Lachnospiraceae bacterium_5_1_63FAA,* and *Barnesiella intestinihominis* were positively associated with ETC1 (mainly PFAS), while in males, abundance of *Bacteroides dorei, Bacteroides vulgatus, Bacteroides ovatus, Bacteroides faeces, Bacteroides xylanisolvens, Veillonella parvula, Ruminococcus lactaris, Escherichia* spp., *Eubacterium eligens, Eubacterium ramulus, Coprococcus comes, Bifidobacterium*

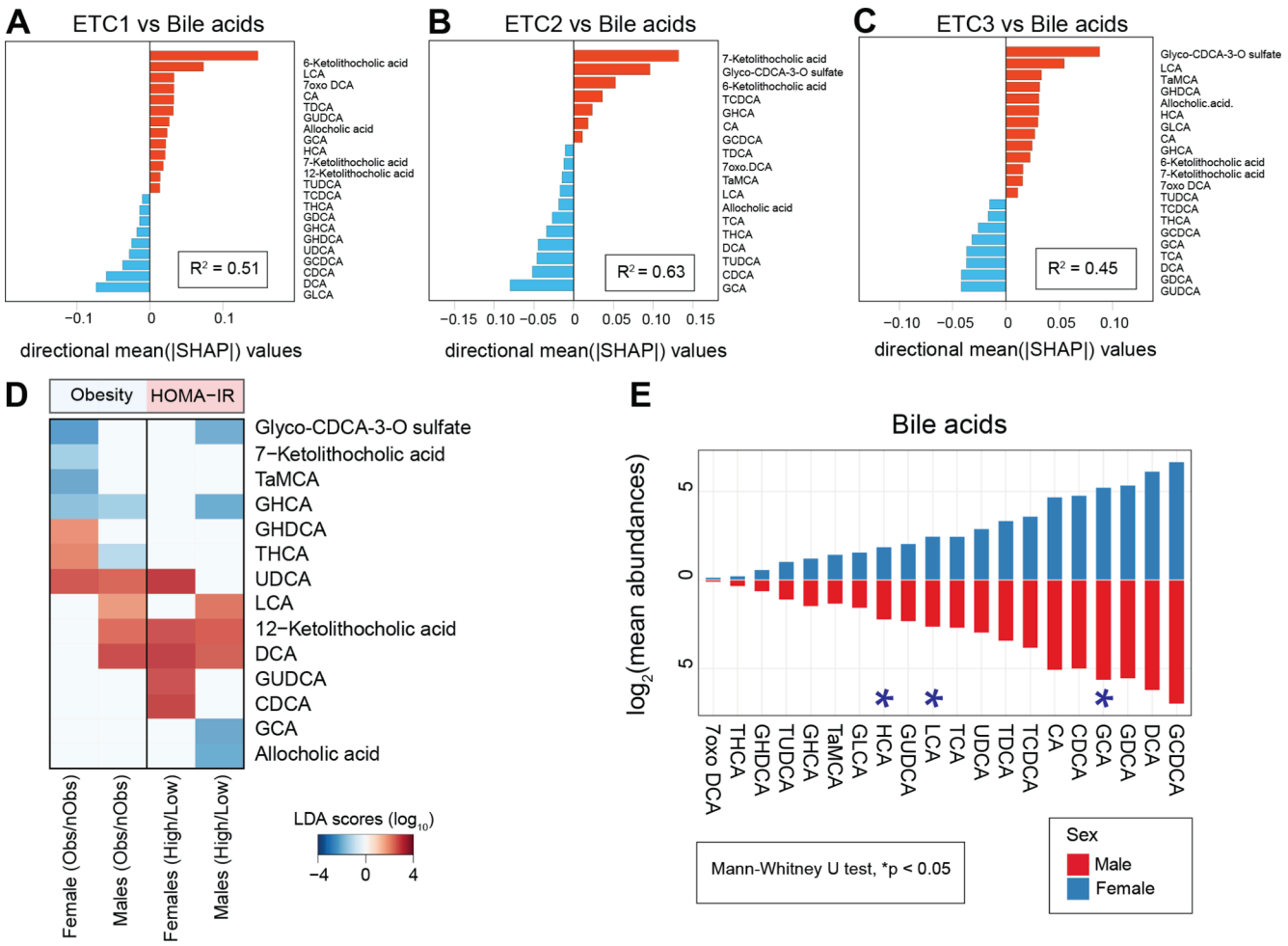

Fig. 2. Environmental toxicant clusters that are linked to serum bile acids. (A-C) The directional mean |SHAP| values of bile acids (BAs) associated with environmental toxicant clusters ETC (1,2,3) respectively, estimated by GBDT–regression models adjusted for the confounding effects of sex and smoking habits of the subjects. The model performances are given as a mean R-squared. '+ve' and '-ve' SHAP values are illustrated by red and blue colors respectively. **(D)** Heatmap showing difference in the serum BA concentrations represented by log (LDA scores) in the obese (Obs) *vs.* non-obese (nObs), and high *vs.* low HOMA-IR in females and males. '+ve' and '-ve' LDA scores are denoted by red and blue colors, respectively. LDA scores that pass the statistical significance (Wilcoxon signed-rank test, $p < 0.05$) are shown. **(E)** A tornado plot showing $\log_2$ mean abundances of BA concentrations in the females and males. (For interpretation of the references to colour in this figure legend, the reader is referred to the web version of this article.)

adolescentis, Bifidobacterium longum, Desulfovibrio desulfuricans, Escherichia spp., *Lachnospiraceae bacterium_{31}_46FAA,* and *Alistipes senegalensis* was positively associated with ETC1 (Fig. 4).

Furthermore, we found that specific gut bacterial species were positively associated with ETC2 and 3. For instance, abundance of *Eubacterium hallii, Bifidobacterium longum, Desulfovibrio desulfuricans, Oxalobacter formigenes, Veillonella atypica, Ruminococcus torques, Streptococcus parasanguinis, Parabacteroides distasonis, Lachnospiraceae bacterium_7_1_58FAA, Holdemania filiformis and Bacteroidales bacterium_ph8* was positively associated with ETC2 in females. Abundance of *Anaerotruncus* spp., *Ruminococcus obeum, Peptostreptococcaceae* spp., *Odoribacter splanchnicus, Pseudoflavonifractor capillosus, Alistipes onderdonkii, Eubacterium rectale, Clostridium leptum, Prevotella copri, Subdoligranulum variabile, Bilophila* spp., *Olsenella* spp., *Bacteroides faecis, Bacteroides cellulosilyticus, Dorea formicigenerans,* and *Roseburia inulinivorans* was positively associated with ETC2 in males (Fig. 4).

Some bacteria such as *Erysipelotrichaceae bacterium_21_3, Ruminococcaceae bacterium_D16, Eubacterium siraeum, Subdoligranulum* spp., *Ruminococcus torques, Parabacteroides distasonis and Barnesiella intestinihominis* was positively associated with ETC3 in females, whilst *Anaerotruncus* spp., *Dorea longicatena, Ruminococcus obeum, Bacteroides dorei, Bacteroides stercoris, Bacteroides caccae, Bacteroides ovatus, Eubacterium ventriosu* and *Coprobacter fastidiosus* was positively associated with ETC3 in males (Fig. 4).

In addition, abundance of *Ruminococcus obeum, Clostridium leptum, Prevotella copri, Bacteroides fragilis, Eubacterium hallii (ETC2), Dorea formicigenerans, Streptococcus salivarius, Bacteroides ovatus,* and *Coprobacter fastidiosus* showed inverse associations with ETCs in females. Conversely, *Ruminococcus sp_5_1_39BFAA, Coprococcus catus, Dorea formicigenerans, Bacteroides cellulosilyticus, Lachnospiraceae bacterium_1_1_57FAA, Haemophilus parainfluenzae, Faecalibacterium prausnitzii, Parasutterella excrementihominis, Clostridium bolteae, Parabacteroides merdae, Roseburia hominis, Streptococcus salivarius, Alistipes senegalensis, Barnesiella intestinihominis, Oscillibacter* spp. *Bacteroidales bacterium_ph8 and Roseburia inulinivorans* showed inverse associations with ETCs in males (Fig. 4).

Notably, several structural variants (SVs) of Coprococcus strains were inversely associated with perfluorodecanoic acid (PFDA). SVs of *Dorea formicigenerans* were positively associated with dPFAM whereas SVs of *Eubacterium siraeum* were inversely associated with dPFAM. In addition, SVs of *Roseburia intestinalis and Ruminococcus* spp. were inversely associated with dPFAmCACEs (**Fig. S8**).

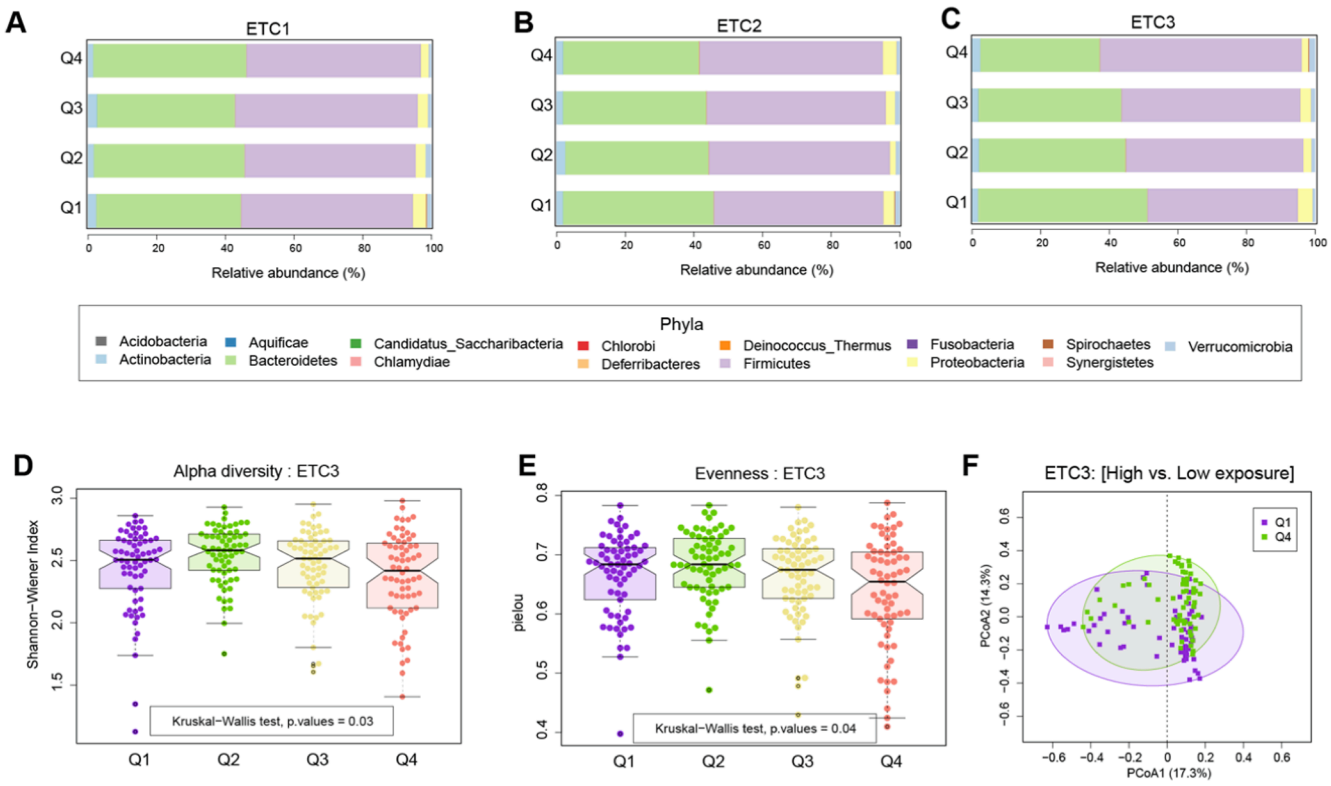

Fig. 3. Differences in the composition and diversity of gut microbiome across various exposure groups. (A-C) shows percentage of relative abundances of microbial phyla in the high (quartiles, Q4), intermediate (Q2-Q3) and low (Q1) exposure groups stratified for ETC (1,2,3) respectively. **(D-E)** Boxplots showing alpha-diversity (*Shannon-Weiner index*), and evenness of the gut microbiome along the exposure groups in ETC3. Dot depicts α-diversity estimated for a sample/subject. A change in the α-diversity was determined by Kruskal–Wallis one-way analysis of variance. **(F)** A score plot showing beta-diversity (principal coordinate analysis, PCoA using Bray-Curtis dissimilarity) of the gut microbiome in the high *vs.* low exposure groups in ETC3. Dot depicts a sample/subject.

3.5. Microbiome-derived secondary bile acids serve as intermediaries between exposures to PFAS and metabolic measures

To investigate the potential causal relationships between ETs (specifically PFAS), gut microbiome-synthesized secondary BAs, and metabolic measures such as obesity, BMI, or HOMA-IR, we performed mediation analysis (**Materials and methods**). We observed that association between PFAS and the metabolic measures was mediated ($p < 0.05$) by secondary BAs. Thereby, secondary BAs likely acted as intermediaries linking PFAS and metabolic measures, with PFDA, PFOA, PFHxS, and PFOS being the prominent contributors (**Fig. S9**).

Additionally, our findings indicate that UDCA might function as a mediator between PFOS and metabolic measures in both males and females. Conversely, in males, LCA appears to mediate the relationship between PFOA or PFOS and metabolic measures, while in females, UDCA showed a mediation effect between Br-PFOS and metabolic measures (**Fig. S9**).

3.6. Microbiome-derived synthesis of BAs may be altered by ETs

To estimate a potential regulation of ETs on microbiome-derived BA synthesis, we developed personalized microbiota models for all 264 study participants. Our current understanding suggests that certain gut bacteria can metabolize BAs, as indicated by (Heinken et al., 2019). Therefore, to develop a microbiota community model, we included genome-scale metabolic models (GEMs) of thirty-one abundant bacterial species (forty-four strains) which have predicted BA metabolizing genes/enzymes and pathway(s) (Heinken et al., 2019; Magnusdottir et al., 2017; Noronha et al., 2019). These bacteria were associated with at least one ETC (Fig. 4). The abundance of metagenomic species was used to contextualize the microbiota community model for each individual (Fig. 4, Fig. 5**A**, **Fig. S10**).

The microbiota model and the metagenomic abundances of the gut bacteria enabled us to estimate the mean relative abundances of BA reactions. As expected, *bile salt hydrolases (BSH)* reactions showed higher relative abundances (%) as compared to the other reaction classes (Fig. 5**B**). The relative abundance of BA reactions was altered by high chemical exposure. Interestingly, these concomitant changes were evident in the reactions facilitated by *3-, 7-, 12-, alpha/beta hydroxysteroid dehydrogenases* (Fig. 5**B-E**). Overall, the relative abundance of *alpha/beta hydroxysteroid dehydrogenases* was higher (Mann-Whitney U test, p-values adjusted for FDR < 0.05) in the high chemical exposure groups (Fig. 5**B-F**). However, the relative abundance of *7-alpha/beta hydroxysteroid dehydrogenase* was markedly lower in the high (*vs.* low) chemical exposure groups associated with ETC2 and 3 (Fig. 5**D**). *7-alpha/beta hydroxysteroid dehydrogenase* catalyzes the conversion of CDCA to UDCA, and a lower reaction potential might, in turn, decrease the formation of UDCA whilst increase the intermediate ketolithocholic acid as discussed above (Fig. 2, Fig. 5**F**).

In addition, Spearman's correlation analysis showed that the abundance of several bacterial species of genus *Alistipes, Bacteroidetes, Clostridium* and *Ruminococcus,* respectively, was positively associated with *7-alpha/beta hydroxysteroid dehydrogenases,* whilst abundance of *Eubacterium* and *Paraprevotella* spp., was inversely associated. In addition, abundance of *Dorea longicatena* and *Roseburia intestinalis* were positively associated with *BSH* (Fig. 5**A**).

3.7. Evidence of alterations in the hepatic LCA to UDCA ratio of humanized PPARα mice following PFOA exposure

Next, we analyzed BA data from a previously conducted exposure study using a humanized PPARα (hPPARα) mouse model (Schlezinger

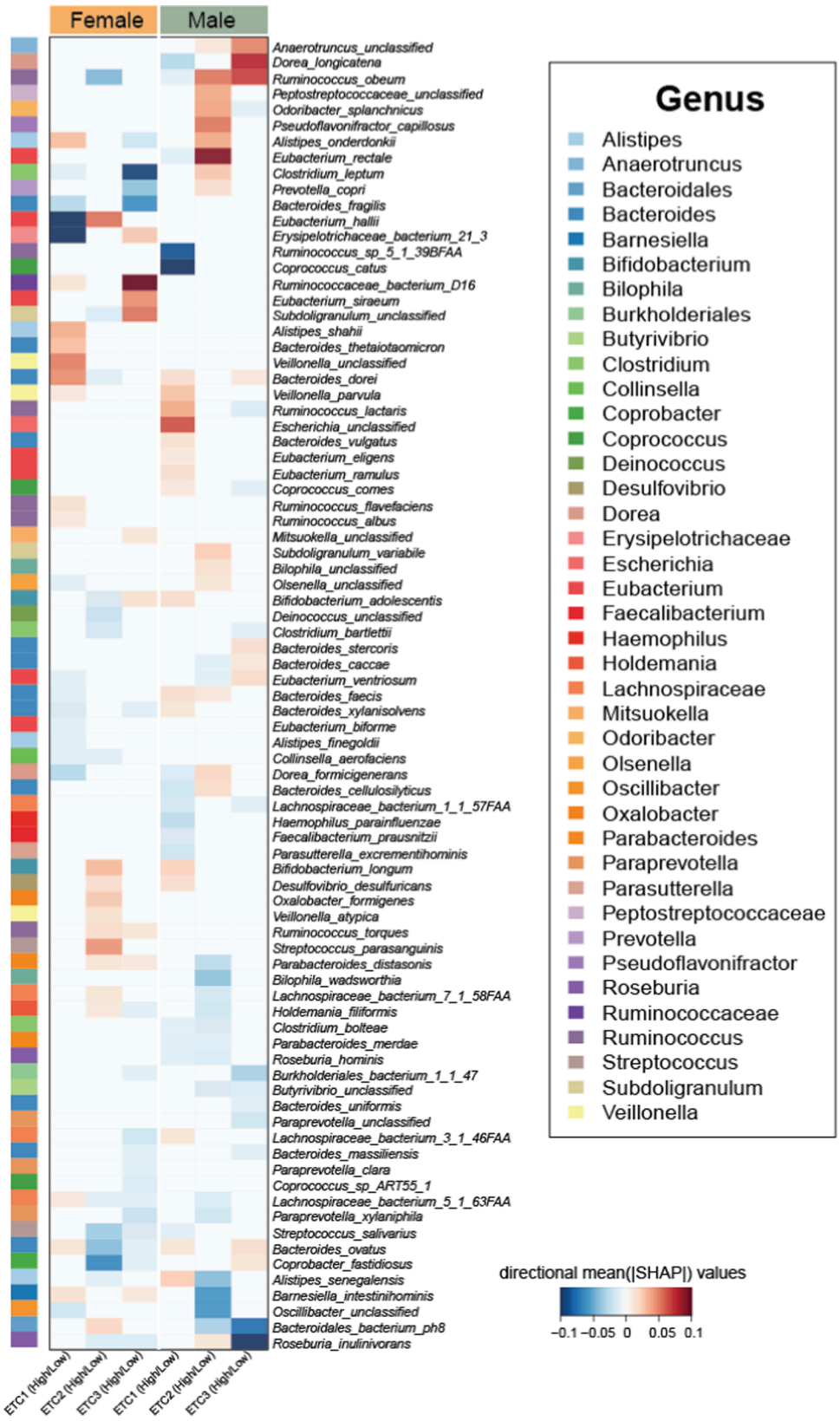

Fig. 4. Gut microbial species that are associated with ETCs in females and males. Heatmap showing the directional mean |SHAP| values of microbial abundances associated with ETCs, estimated by the GBDT–regression models adjusted for the confounding effects of sex and smoking habit of the subjects. '+ve' and '-ve' SHAP values are illustrated by red and blue colors respectively. (For interpretation of the references to colour in this figure legend, the reader is referred to the web version of this article.)

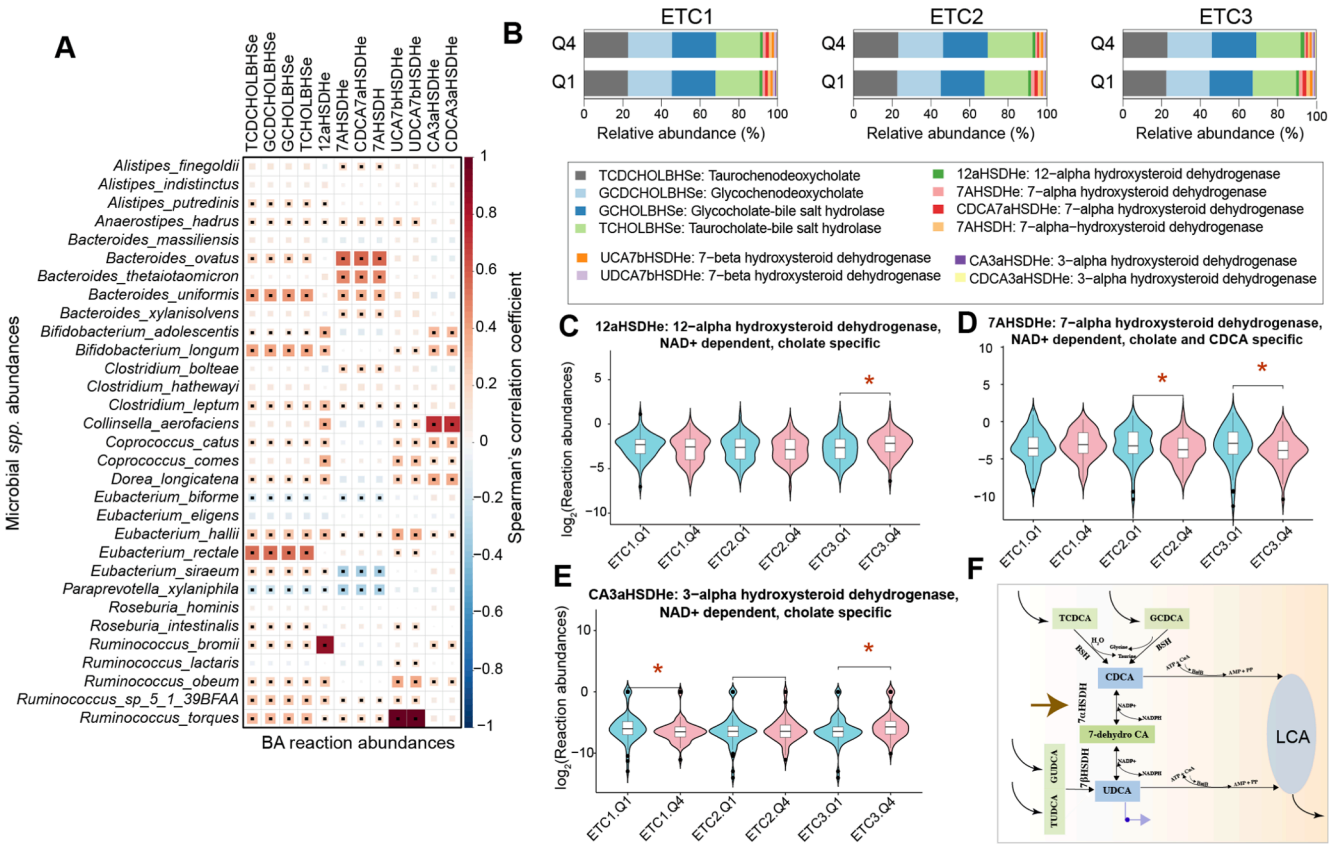

Fig. 5. Dysregulation of BA pathways following chemical exposure. (A) A Heatmap showing Spearman's correlation coefficients between BA reaction abundances (community microbiota models) *vs.* microbial spp. Positive and negative associations are illustrated by red and blue colors respectively. **(B)** Shows percentage of relative abundances of BA reactions in the high (quartiles, Q4), and low (Q1) exposure groups stratified for ETC (1,2,3), respectively. **(C-E)** Violin plots showing the distribution of abundances of BA reactions in high and low exposure groups of the ETCs. **(F)** A pathway Illustration showing interconversion of CDCA to UDCA and LCA. *p < 0.05 (adjusted for FDR). (For interpretation of the references to colour in this figure legend, the reader is referred to the web version of this article.)

et al., 2021; Schlezinger et al., 2020). We thereby sought to explore if changes in the LCA to UDCA ratios were intrinsically linked to chemical exposure. Male and female hPPARα mice were exposed to vehicle (VH, 0.5 % sucrose) or PFOA at a concentration of 8 μM of PFOA (3.5 mg/L) in drinking water *ad libitum* for 6–7 weeks and fed a Western type of diet, resulting in average plasma levels of ca. 48 μg/mL of PFOA (Schlezinger et al., 2021). In energy percentage, the diet contained 51.8 % carbohydrate, 33.5 % fat, and 14.7 % protein. The relatively high serum PFOA levels in mice, corresponding to those found in highly exposed humans, were chosen to account for the substantially shorter half-life of PFOA in mice compared with humans (Schlezinger et al., 2021).

Hepatic BAs were measured in two groups, PFOA (n = 8 mice; 5 female mice) and vehicle (VH) (n = 8 mice; 4 female mice) exposure, respectively. The ratios of LCA/UDCA were significantly elevated in both female and male mice groups treated with PFOA *vs.* VH (Fig. 6). Thus, the outcome of studies in the animal model supports our findings from the human cohort that chemical exposure, particularly exposure to PFAS, may elevate LCA to UDCA ratio, which is likely linked to obesity and insulin resistance.

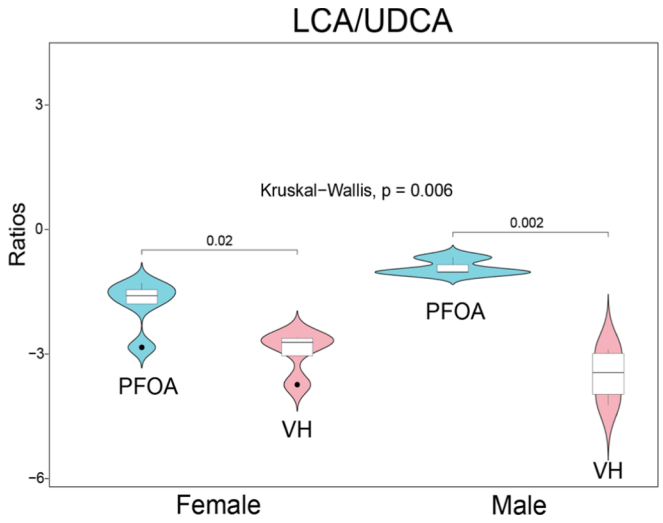

Fig. 6. Hepatic LCA/UDCA ratio in hPPARα mice associated with chemical exposure. Difference (Kruskal − Wallis test, statistical significance at nominal p-value < 0.05) in the UDCA/LCA ratios of PFOA (n = 8; 5 females and 3 males) *vs.* vehicle (VH; n = 8; 4 females and 4 males) administered mice groups.

4. Discussion

We examined the relationships between serum concentration of ETs, composition of gut microbiota, serum BAs, measures of insulin resistance and obesity in Danish adults. In addition to traditional PFAS (*e.g.*, PFOS, PFOA, PFHxS) we could detect other organofluorine compounds, the latter by using suspect screening approach. While the identification of the latter could not be verified with authentic standards as these are not available, we did observe significant correlation with them and the target PFAS, both supporting their identification as well as suggesting similar exposure sources. Our results suggest that exposure to ETs is associated with gut dysbiosis and altered fasting BA pool, which, in turn, is linked to obesity and insulin resistance.

So far, only a few human studies have investigated a potential relationship between ETs and the gut microbiome composition and function, and even fewer studies have explored interplays between serum concentration of ETs, gut microbiome, serum metabolites and metabolic health. These studies have associated elevated PFAS exposures with distinct bacterial taxa (Gardner et al., 2021; Thompson et al., 2022). Importantly, our results indicate that higher chemical exposure is associated with a higher Firmicutes to Bacteroides ratio (F/B). A high F/B ratio has previously been linked with gut dysbiosis and obesity (Ley et al., 2006; Stojanov et al., 2020). We also identified several bacterial spp. of genus *Roseburia, Subdoligranulum, Dorea, Ruminococcus, Eubacterium, Veillonella and Clostridium* to be associated with high chemical exposure. This is in agreement with a study that reported an increase in abundance of *Dorea longicatena* with exposure to PFOS (Thompson et al., 2022). Higher abundance of some of the mentioned gut bacteria are considered biomarkers of obesity and/or insulin resistance (Chakraborti, 2015; Ley et al., 2006; Schneeberger et al., 2015).

We have previously reported that *Prevotella copri* and *Bacteroides vulgatus* are associated with obesity, insulin resistance, and biosynthesis of specific metabolites such as branched-chain amino acids, tryptophan, and lipopolysaccharides (Pedersen et al., 2016) that may be implicated in metabolic disorders. Here, we found that high chemical exposure was correlated with higher abundance of these bacteria in males, while *Prevotella copri* showed inverse association with chemical exposure in females. Overall, males had higher abundance of *Prevotella copri* than females. Several other studies have suggested a link between *Prevotella* diversity and human health, with both positive and negative associations reported, potentially due to the complex interaction various *Prevotella copri* strains and differences in habitual diet (Tett et al., 2021). Specifically, fiber-rich diets associated with *Prevotella copri* showed beneficial health impacts while *Prevotella copri* strains associated with an omnivore diet were linked with increased glucose intolerance and type 2 diabetes (De Filippis et al., 2019). As several of ETs are bioaccumulated in animal-based fat products, a relative high ET content of predominantly fatty animal-based food might be an additional driver of the adverse health impact of this widespread food habit in the western world.

We found that exposure to ETs was associated with elevated circulating levels of microbiome-derived LCA and decreased serum levels of UDCA, further suggesting that ETs might induce dysbiosis in the gut microbiome affecting the conversion of secondary BAs. The serum BA pool is regulated *via* the hepatic FXR that has a central role in regulation of BA synthesis and secretion as well as in the regulation of lipid and glucose homeostasis in the liver (Gao et al., 2022; Gonzalez et al., 2016). Remarkably, LCA and UDCA have opposite impact on FXR, with LCA being an agonist while UDCA an antagonist. Indeed, mediation analysis suggested that the secondary BAs might act as potential mediators of insulin resistance. In the present study, obese males with poor insulin sensitivity had higher serum concentrations of LCA and PFAS as compared to their non-obese male counterparts as well as to females, suggesting that especially highly PFAS-exposed males are more susceptible to metabolic dysregulation. However, the mediation analysis of the effect of PFAS on the HOMA-IR and gut-derived BAs was stronger in females than in males, suggesting that this could be one of the factors in sex-specific differences in the impact of exposure. The finding aligns with previous studies, showing a sexually dimorphic pattern of ET exposures in metabolic disorders (Schlezinger et al., 2020; Sen et al., 2022).

Recently, murine studies showed that UDCA may alleviate metabolic dysfunction and could have a potential role in the prevention or treatment of obesity (Zhang et al., 2019). In addition, UDCA has been suggested as a treatment for MASLD (Kosmalski et al., 2023). Interestingly, the LCA/UDCA ratio was increased in our PPARα-humanized murine model exposed to PFOA. Moreover, personalized community modeling of the gut microbiota identified a downregulation of the *7-alpha-hydroxysteroid dehydrogenase* pathway in the high chemical exposure groups that is involved in the biotransformation of CDCA to UDCA. Several bacterial spp. of genus *Bacteroidetes, Clostridium, Ruminococcus* and *Eubacterium* were positively associated with this pathway. In this context it is of interest that higher abundance of *Ruminococcus* and *Bacteroidetes* have been associated with obesity and other metabolic diseases (Gentile et al., 2022). Therefore, LCA/UDCA ratio may be one of the determinants of insulin sensitivity in the high ET exposure groups. A high level of serum LCA may cause hepatotoxicity (Zhao et al., 2017), and it has also been linked with increased susceptibility of metabolic diseases such as MASLD, type 2 diabetes and the metabolic syndrome (Grzych et al., 2021; Masoodi et al., 2021). Future long-term mechanistic studies of the implications on development of dys-metabolic states following PFAS induced altered LCA/UDCA ratio are needed.

In summary, our study on Danish adults reveals a significant link between exposure to endocrine disruptors (ETs), gut microbiome imbalance, and alterations in serum bile acids. This disturbance is associated with obesity and insulin resistance. We found sex-specific variations in bacterial abundances and identified a potential role of microbiome-derived secondary BAs as mediators of insulin resistance. These findings emphasize the impact of ETs, such as PFAS, on metabolic health in a sexually dimorphic manner. Further research is needed to explore mechanistic implications and long-term effects.

CRediT authorship contribution statement

Partho Sen: Writing – review & editing, Writing – original draft, Methodology, Formal analysis, Data curation. **Yong Fan:** Writing – review & editing, Formal analysis. **Jennifer J. Schlezinger:** Writing – review & editing, Investigation. **Stanislav D. Ehrlich:** Writing – review & editing, Resources. **Thomas F. Webster:** Writing – review & editing, Investigation. **Tuulia Hyötyläinen:** Writing – review & editing, Writing – original draft, Supervision, Resources, Investigation, Conceptualization. **Oluf Pedersen:** Writing – review & editing, Writing – original draft, Supervision, Resources, Conceptualization. **Matej Orešič:** Writing – review & editing, Writing – original draft, Supervision, Conceptualization.

Declaration of competing interest

The authors declare the following financial interests/personal relationships which may be considered as potential competing interests: Matej Oresic reports financial support was provided by Research Council of Finland. Tuulia Hyotylainen reports financial support was provided by Novo Nordisk Foundation. Tuulia Hyotylainen reports financial support was provided by Swedish Research Council Formas. Tuulia Hyotylainen reports financial support was provided by Swedish Research Council. If there are other authors, they declare that they have no known competing financial interests or personal relationships that could have appeared to influence the work reported in this paper.

Data availability

Link to data provided

Acknowledgements

The present work was supported by Academy of Finland (grant no. 333981 to M.O.), Novo Nordisk Foundation (grants no. NNF20OC0063971 and NNF21OC0070309 to T.H.), Swedish Research Council (grant no. and 2020-03674 to T.H and M.O), Formas (grant no. 2019-00869 to T.H and M.O). The Novo Nordisk Foundation Center for Basic Metabolic Research is an independent research institution at the University of Copenhagen, partially funded by an unrestricted donation from the Novo Nordisk Foundation. The funders had no role in the study design nor in the collection, analysis, and interpretation of data.

Appendix A. Supplementary material

Supplementary data to this article can be found online at https://doi.org/10.1016/j.envint.2024.108569.

References

Ammitzbøll, C., Börnsen, L., Petersen, E.R., Oturai, A.B., Søndergaard, H.B., Grandjean, P., Sellebjerg, F., 2019. Perfluorinated substances, risk factors for multiple sclerosis and cellular immune activation. J. Neuroimmunol. 330, 90–95.

Andersen, M.E.; Hagenbuch, B.; Apte, U.; Corton, J.C.; Fletcher, T.; Lau, C.; Roth, W.L.; Staels, B.; Vega, G.L.; Clewell, H.J., 3rd; Longnecker, M.P. Why is elevation of serum cholesterol associated with exposure to perfluoroalkyl substances (PFAS) in humans? A workshop report on potential mechanisms. Toxicology 2021;459:152845.

Armstrong, L.E., Guo, G.L., 2019. Understanding environmental contaminants' direct effects on non-alcoholic fatty liver disease progression. Curr. Environ. Health Rep. 6, 95–104.

Beggs, K.M., McGreal, S.R., McCarthy, A., Gunewardena, S., Lampe, J.N., Lau, C., Apte, U., 2016. The role of hepatocyte nuclear factor 4-alpha in perfluorooctanoic acid- and perfluorooctanesulfonic acid-induced hepatocellular dysfunction. Toxicol. Appl. Pharmacol. 304, 18–29.

Behr, A.C., Kwiatkowski, A., Stahlman, M., Schmidt, F.F., Luckert, C., Braeuning, A., Buhrke, T., 2020b. Impairment of bile acid metabolism by perfluorooctanoic acid (PFOA) and perfluorooctanesulfonic acid (PFOS) in human HepaRG hepatoma cells. Arch. Toxicol. 94, 1673–1686.

Behr, A.-C., Plinsch, C., Braeuning, A., Buhrke, T., 2020a. Activation of human nuclear receptors by perfluoroalkylated substances (PFAS). Toxicol. In Vitro 62, 104700.

Cardenas, A., Gold, D.R., Hauser, R., Kleinman, K.P., Hivert, M.-F., Calafat, A.M., Ye, X., Webster, T.F., Horton, E.S., Oken, E., 2017. Plasma concentrations of per- and polyfluoroalkyl substances at baseline and associations with glycemic indicators and diabetes incidence among high-risk adults in the diabetes prevention program trial. Environ. Health Perspect. 125, 107001.

Chakraborti, C.K., 2015. New-found link between microbiota and obesity. World J. Gastrointest. Pathophysiol. 6, 110–119.

Chiu, K., Warner, G., Nowak, R.A., Flaws, J.A., Mei, W., 2020. The impact of environmental chemicals on the gut microbiome. Toxicol. Sci. 176, 253–284.

Christensen, K.Y., Raymond, M., Meiman, J., 2019. Perfluoroalkyl substances and metabolic syndrome. Int. J. Hyg. Environ. Health 222, 147–153.

Claus, S.P., Guillou, H., Ellero-Simatos, S., 2016. The gut microbiota: A major player in the toxicity of environmental pollutants? NPJ Biofilms Microbiomes 2, 16003.

De Filippis, F., Pasolli, E., Tett, A., Tarallo, S., Naccarati, A., De Angelis, M., Neviani, E., Cocolin, L., Gobbetti, M., Segata, N., Ercolini, D., 2019. Distinct genetic and functional traits of human intestinal Prevotella copri strains are associated with different habitual diets. Cell Host Microbe 25 (444–453), e443.

Deierlein, A.L., Rock, S., Park, S., 2017. Persistent endocrine-disrupting chemicals and fatty liver disease. Curr. Environ. Health Rep. 4, 439–449.

Fenton, S.E., Ducatman, A., Boobis, A., DeWitt, J.C., Lau, C., Ng, C., Smith, J.S., Roberts, S.M., 2021. Per- and polyfluoroalkyl substance toxicity and human health review: Current state of knowledge and strategies for informing future research. Environ. Toxicol. Chem. 40, 606–630.

Fromentin, S., Forslund, S.K., Chechi, K., Aron-Wisnewsky, J., Chakaroun, R., Nielsen, T., Tremaroli, V., Ji, B., Prifti, E., Myridakis, A., Chilloux, J., Andrikopoulos, P., Fan, Y., Olanipekun, M.T., Alves, R., Adiouch, S., Bar, N., Talmor-Barkan, Y., Belda, E., Caesar, R., Coelho, L.P., Falony, G., Fellahi, S., Galan, P., Galleron, N., Helft, G., Hoyles, L., Isnard, R., Le Chatelier, E., Julienne, H., Olsson, L., Pedersen, H.K., Pons, N., Quinquis, B., Rouault, C., Roume, H., Salem, J.E., Schmidt, T.S.B., Vieira-Silva, S., Li, P., Zimmermann-Kogadeeva, M., Lewinter, C., Sondertoft, N.B., Hansen, T.H., Gauguier, D., Gotze, J.P., Kober, L., Kornowski, R., Vestergaard, H., Hansen, T., Zucker, J.D., Hercberg, S., Letunic, I., Backhed, F., Oppert, J.M., Nielsen, J., Raes, J., Bork, P., Stumvoll, M., Segal, E., Clement, K., Dumas, M.E., Ehrlich, S.D., Pedersen, O., 2022. Microbiome and metabolome features of the cardiometabolic disease spectrum. Nat. Med. 28, 303–314.

Gao, R., Meng, X., Xue, Y., Mao, M., Liu, Y., Tian, X., Sui, B., Li, X., Zhang, P., 2022. Bile acids-gut microbiota crosstalk contributes to the improvement of type 2 diabetes mellitus. Front. Pharmacol. 13, 1027212.

Gardner, C.M., Hoffman, K., Stapleton, H.M., Gunsch, C.K., 2021. Exposures to semivolatile organic compounds in indoor environments and associations with the gut microbiomes of children. Environ. Sci. Technol. Lett. 8, 73–79.

Geng, D., Musse, A.A., Wigh, V., Carlsson, C., Engwall, M., Oresic, M., Scherbak, N., Hyotylainen, T., 2019. Effect of perfluorooctanesulfonic acid (PFOS) on the liver lipid metabolism of the developing chicken embryo. Ecotoxicol. Environ. Saf. 170, 691–698.

Gentile, J.K.A., Oliveira, K.D., Pereira, J.G., Tanaka, D.Y., Guidini, G.N., Cadona, M.Z., Siriani-Ribeiro, D.W., Perondini, M.T., 2022. The intestinal microbiome in patients undergoing bariatric surgery: A systematic review. Arq. Bras. Cir. Dig. 35, e1707.

Gonzalez, F.J., Jiang, C., Patterson, A.D., 2016. An intestinal microbiota-farnesoid X receptor axis modulates metabolic disease. Gastroenterology 151, 845–859.

Grzych, G., Chavez-Talavera, O., Descat, A., Thuillier, D., Verrijken, A., Kouach, M., Legry, V., Verkindt, H., Raverdy, V., Legendre, B., Caiazzo, R., Van Gaal, L., Goossens, J.F., Paumelle, R., Francque, S., Pattou, F., Haas, J.T., Tailleux, A., Staels, B., 2021. NASH-related increases in plasma bile acid levels depend on insulin resistance. JHEP Rep. 3, 100222.

Guzior, D.V., Quinn, R.A., 2021. Review: Microbial transformations of human bile acids. Microbiome 9, 140.

Heinken, A., Ravcheev, D.A., Baldini, F., Heirendt, L., Fleming, R.M.T., Thiele, I., 2019. Systematic assessment of secondary bile acid metabolism in gut microbes reveals distinct metabolic capabilities in inflammatory bowel disease. Microbiome 7, 75.

Heinken, A., Hertel, J., Acharya, G., Ravcheev, D.A., Nyga, M., Okpala, O.E., Hogan, M., Magnusdottir, S., Martinelli, F., Nap, B., Preciat, G., Edirisinghe, J.N., Henry, C.S., Fleming, R.M.T., Thiele, I., 2023. Genome-scale metabolic reconstruction of 7,302 human microorganisms for personalized medicine. Nat. Biotechnol.

Hyotylainen, T., McGlinchey, A., Salihovic, S., Schubert, A., Douglas, A., Hay, D.C., O'Shaughnessy, P.J., Iredale, J.P., Shaw, S., Fowler, P.A., Oresic, M., 2024. In utero exposures to perfluoroalkyl substances and the human fetal liver metabolome in Scotland: A cross-sectional study. Lancet Planet Health 8, e5–e17.

Jin, Y., Wu, S., Zeng, Z., Fu, Z., 2017. Effects of environmental pollutants on gut microbiota. Environ. Pollut. 222, 1–9.

Ke, G., Meng, Q., Finley, T., Wang, T., Chen, W., Ma, W., Ye, Q., Liu, T.-Y., 2017. Lightgbm: A highly efficient gradient boosting decision tree. Adv. Neural Inf. Proces. Syst. 30.

Kosmalski, M., Frankowski, R., Ziolkowska, S., Rozycka-Kosmalska, M., Pietras, T., 2023. What's new in the treatment of non-alcoholic fatty liver disease (NAFLD). J. Clin. Med. 12.

Lai, K.P., Ng, A.H., Wan, H.T., Wong, A.Y., Leung, C.C., Li, R., Wong, C.K., 2018. Dietary exposure to the environmental chemical, PFOS on the diversity of gut microbiota, associated with the development of metabolic syndrome. Front. Microbiol. 9, 2552.

Lamichhane, S., Sen, P., Dickens, A.M., Alves, M.A., Harkonen, T., Honkanen, J., Vatanen, T., Xavier, R.J., Hyotylainen, T., Knip, M., Oresic, M., 2022. Dysregulation of secondary bile acid metabolism precedes islet autoimmunity and type 1 diabetes. Cell Rep. Med. 3, 100762.

Le Chatelier, E.; Nielsen, T.; Qin, J.; Prifti, E.; Hildebrand, F.; Falony, G.; Almeida, M.; Arumugam, M.; Batto, J.M.; Kennedy, S.; Leonard, P.; Li, J.; Burgdorf, K.; Grarup, N.; Jorgensen, T.; Brandslund, I.; Nielsen, H.B.; Juncker, A.S.; Bertalan, M.; Levenez, F.; Pons, N.; Rasmussen, S.; Sunagawa, S.; Tap, J.; Tims, S.; Zoetendal, E.G.; Brunak, S.; Clement, K.; Dore, J.; Kleerebezem, M.; Kristiansen, K.; Renault, P.; Sicheritz-Ponten, T.; de Vos, W.M.; Zucker, J.D.; Raes, J.; Hansen, T.; Meta, H.I.T.c.; Bork, P.; Wang, J.; Ehrlich, S.D.; Pedersen, O. Richness of human gut microbiome correlates with metabolic markers. Nature 2013;500:541-546.

Ley, R.E., Turnbaugh, P.J., Klein, S., Gordon, J.I., 2006. Microbial ecology: human gut microbes associated with obesity. Nature 444, 1022–1023.

Louisse, J., Fragki, S., Rijkers, D., Janssen, A., van Dijk, B., Leenders, L., Staats, M., Bokkers, B., Zeilmaker, M., Piersma, A., Luijten, M., Hoogenboom, R., Peijnenburg, A., 2023. Determination of in vitro hepatotoxic potencies of a series of perfluoroalkyl substances (PFASs) based on gene expression changes in HepaRG liver cells. Arch. Toxicol. 97, 1113–1131.

Lundberg, S.M.; Erion, G.G.; Lee, S.-I. Consistent Individualized Feature Attribution for Tree Ensembles. ArXiv 2018;abs/1802.03888.

Magnusdottir, S., Heinken, A., Kutt, L., Ravcheev, D.A., Bauer, E., Noronha, A., Greenhalgh, K., Jager, C., Baginska, J., Wilmes, P., Fleming, R.M., Thiele, I., 2017. Generation of genome-scale metabolic reconstructions for 773 members of the human gut microbiota. Nat. Biotechnol. 35, 81–89.

Masoodi, M., Gastaldelli, A., Hyotylainen, T., Arretxe, E., Alonso, C., Gaggini, M., Brosnan, J., Anstee, Q.M., Millet, O., Ortiz, P., Mato, J.M., Dufour, J.F., Oresic, M., 2021. Metabolomics and lipidomics in NAFLD: Biomarkers and non-invasive diagnostic tests. Nat. Rev. Gastroenterol. Hepatol. 18, 835–856.

McGlinchey, A.; Sinioja, T.; Lamichhane, S.; Bodin, J.; Siljander, H.; Geng, D.; Carlsson, C.; Duberg, D.; Ilonen, J.; Virtanen, S.M.; Dirven, H.; Bernstsen, H.F.; Zimmer, K.; Nygaard, U.C.; Orešič, M.; Knip, M.; Hyötyläinen, T. Prenatal Exposure To Environmental Chemicals Modulates Serum Phospholipids In Newborn Infants, Increasing Later Risk Of Type 1 Diabetes. bioRxiv 2019:588350.

Nielsen, F., Fischer, F.C., Leth, P.M., Grandjean, P., 2024. Occurrence of major perfluorinated alkylate substances in human blood and target organs. Environ. Sci. Technol. 58, 143–149.

Noronha, A., Modamio, J., Jarosz, Y., Guerard, E., Sompairac, N., Preciat, G., Danielsdottir, A.D., Krecke, M., Merten, D., Haraldsdottir, H.S., Heinken, A., Heirendt, L., Magnusdottir, S., Ravcheev, D.A., Sahoo, S., Gawron, P., Friscioni, L., Garcia, B., Prendergast, M., Puente, A., Rodrigues, M., Roy, A., Rouquaya, M., Wiltgen, L., Zagare, A., John, E., Krueger, M., Kuperstein, I., Zinovyev, A., Schneider, R., Fleming, R.M.T., Thiele, I., 2019. The virtual metabolic human database: Integrating human and gut microbiome metabolism with nutrition and disease. Nucleic Acids Res. 47, D614–D624.

Oresic, M., McGlinchey, A., Wheelock, C.E., Hyotylainen, T., 2020. Metabolic signatures of the exposome-quantifying the impact of exposure to environmental chemicals on human health. Metabolites 10, 454.

Pandak, W.M., Kakiyama, G., 2019. The acidic pathway of bile acid synthesis: Not just an alternative pathway. Liver Res. 3, 88–98.

Pedersen, H.K., Gudmundsdottir, V., Nielsen, H.B., Hyotylainen, T., Nielsen, T., Jensen, B.A., Forslund, K., Hildebrand, F., Prifti, E., Falony, G., Le Chatelier, E., Levenez, F., Dore, J., Mattila, I., Plichta, D.R., Poho, P., Hellgren, L.I., Arumugam, M., Sunagawa, S., Vieira-Silva, S., Jorgensen, T., Holm, J.B., Trost, K., Meta, H.I.T.C., Kristiansen, K., Brix, S., Raes, J., Wang, J., Hansen, T., Bork, P., Brunak, S., Oresic, M., Ehrlich, S.D., Pedersen, O., 2016. Human gut microbes impact host serum metabolome and insulin sensitivity. Nature 535, 376–381.

Petersen, A.O., Julienne, H., Hyotylainen, T., Sen, P., Fan, Y., Pedersen, H.K., Jantti, S., Hansen, T.H., Nielsen, T., Jorgensen, T., Hansen, T., Myers, P.N., Nielsen, H.B., Ehrlich, S.D., Oresic, M., Pedersen, O., 2021. Conjugated C-6 hydroxylated bile acids in serum relate to human metabolic health and gut Clostridia species. Sci. Rep. 11, 13252.

Qi, W., Clark, J.M., Timme-Laragy, A.R., Park, Y., 2020. Per- and polyfluoroalkyl substances and obesity, type 2 diabetes and non-alcoholic fatty liver disease: A review of epidemiologic findings. Toxicol. Environ. Chem. 102, 1–36.

R Development Core Team. R: A language and environment for statistical computing. Vienna: R Foundation for Statistical Computing; 2018.

Rantakokko, P., Männistö, V., Airaksinen, R., Koponen, J., Viluksela, M., Kiviranta, H., Pihlajamäki, J., 2015. Persistent organic pollutants and non-alcoholic fatty liver disease in morbidly obese patients: a cohort study. Environ. Health 14, 79.

Salihović, S., Dickens, A.M., Schoultz, I., Fart, F., Sinisalu, L., Lindeman, T., Halfvarson, J., Orešič, M., Hyötyläinen, T., 2019. Simultaneous determination of perfluoroalkyl substances and bile acids in human serum using ultra-high-performance liquid chromatography–tandem mass spectrometry. Anal. Bioanal. Chem.

Salihovic, S., Dickens, A.M., Schoultz, I., Fart, F., Sinisalu, L., Lindeman, T., Halfvarson, J., Oresic, M., Hyotylainen, T., 2020. Simultaneous determination of perfluoroalkyl substances and bile acids in human serum using ultra-high-performance liquid chromatography-tandem mass spectrometry. Anal. Bioanal. Chem. 412, 2251–2259.

Schlezinger, J.J., Puckett, H., Oliver, J., Nielsen, G., Heiger-Bernays, W., Webster, T.F., 2020. Perfluorooctanoic acid activates multiple nuclear receptor pathways and skews expression of genes regulating cholesterol homeostasis in liver of humanized PPARalpha mice fed an American diet. Toxicol. Appl. Pharmacol. 405, 115204.

Schlezinger, J.J., Hyotylainen, T., Sinioja, T., Boston, C., Puckett, H., Oliver, J., Heiger-Bernays, W., Webster, T.F., 2021. Perfluorooctanoic acid induces liver and serum dyslipidemia in humanized PPARalpha mice fed an American diet. Toxicol. Appl. Pharmacol. 426, 115644.

Schneeberger, M., Everard, A., Gomez-Valades, A.G., Matamoros, S., Ramirez, S., Delzenne, N.M., Gomis, R., Claret, M., Cani, P.D., 2015. Akkermansia muciniphila inversely correlates with the onset of inflammation, altered adipose tissue metabolism and metabolic disorders during obesity in mice. Sci. Rep. 5, 16643.

Segata, N., Izard, J., Waldron, L., Gevers, D., Miropolsky, L., Garrett, W.S., Huttenhower, C., 2011. Metagenomic biomarker discovery and explanation. Genome Biol. 12, R60.

Segata, N., Waldron, L., Ballarini, A., Narasimhan, V., Jousson, O., Huttenhower, C., 2012. Metagenomic microbial community profiling using unique clade-specific marker genes. Nat. Methods 9, 811–814.

Sen, P., Qadri, S., Luukkonen, P.K., Ragnarsdottir, O., McGlinchey, A., Jantti, S., Juuti, A., Arola, J., Schlezinger, J.J., Webster, T.F., Oresic, M., Yki-Jarvinen, H., Hyotylainen, T., 2021. Exposure to environmental contaminants is associated with altered hepatic lipid metabolism in non-alcoholic fatty liver disease. J. Hepatol.

Sen, P., Qadri, S., Luukkonen, P.K., Ragnarsdottir, O., McGlinchey, A., Jantti, S., Juuti, A., Arola, J., Schlezinger, J.J., Webster, T.F., Oresic, M., Yki-Jarvinen, H., Hyotylainen, T., 2022. Exposure to environmental contaminants is associated with altered hepatic lipid metabolism in non-alcoholic fatty liver disease. J. Hepatol. 76, 283–293.

Sinioja, T., Bodin, J., Duberg, D., Dirven, H., Berntsen, H.F., Zimmer, K., Nygaard, U.C., Oresic, M., Hyotylainen, T., 2022. Exposure to persistent organic pollutants alters the serum metabolome in non-obese diabetic mice. Metabolomics 18, 87.

Stojanov, S.; Berlec, A.; Strukelj, B. The Influence of Probiotics on the Firmicutes/Bacteroidetes Ratio in the Treatment of Obesity and Inflammatory Bowel disease. Microorganisms 2020;8.

Tett, A., Pasolli, E., Masetti, G., Ercolini, D., Segata, N., 2021. Prevotella diversity, niches and interactions with the human host. Nat. Rev. Microbiol. 19, 585–599.

Thompson, K.N., Oulhote, Y., Weihe, P., Wilkinson, J.E., Ma, S., Zhong, H., Li, J., Kristiansen, K., Huttenhower, C., Grandjean, P., 2022. Effects of lifetime exposures to environmental contaminants on the adult gut microbiome. Environ. Sci. Technol. 56, 16985–16995.

Truong, D.T., Franzosa, E.A., Tickle, T.L., Scholz, M., Weingart, G., Pasolli, E., Tett, A., Huttenhower, C., Segata, N., 2015. MetaPhlAn2 for enhanced metagenomic taxonomic profiling. Nat. Methods 12, 902–903.

Wahlstrom, A., Sayin, S.I., Marschall, H.U., Backhed, F., 2016. Intestinal crosstalk between bile acids and Microbiota and its impact on host metabolism. Cell Metab. 24, 41–50.

Wang, D., Doestzada, M., Chen, L., Andreu-Sanchez, S., van den Munckhof, I.C.L., Augustijn, H.E., Koehorst, M., Ruiz-Moreno, A.J., Bloks, V.W., Riksen, N.P., Rutten, J.H.W., Joosten, L.A.B., Netea, M.G., Wijmenga, C., Zhernakova, A., Kuipers, F., Fu, J., 2021. Characterization of gut microbial structural variations as determinants of human bile acid metabolism. Cell Host Microbe 29 (1802–1814), e1805.

Wang, C., Zhang, Y., Deng, M., Wang, X., Tu, W., Fu, Z., Jin, Y., 2019. Bioaccumulation in the gut and liver causes gut barrier dysfunction and hepatic metabolism disorder in mice after exposure to low doses of OBS. Environ. Int. 129, 279–290.

Yu, H., Nie, R., Shen, C., 2023. The role of bile acids in regulating glucose and lipid metabolism. Endocr. J. 70, 359–374.

Zeevi, D., Korem, T., Godneva, A., Bar, N., Kurilshikov, A., Lotan-Pompan, M., Weinberger, A., Fu, J., Wijmenga, C., Zhernakova, A., Segal, E., 2019. Structural variation in the gut microbiome associates with host health. Nature 568, 43–48.

Zhang, L., Rimal, B., Nichols, R.G., Tian, Y., Smith, P.B., Hatzakis, E., Chang, S.C., Butenhoff, J.L., Peters, J.M., Patterson, A.D., 2020. Perfluorooctane sulfonate alters gut microbiota-host metabolic homeostasis in mice. Toxicology 431, 152365.

Zhang, Y., Zheng, X., Huang, F., Zhao, A., Ge, K., Zhao, Q., Jia, W., 2019. Ursodeoxycholic acid alters bile acid and fatty acid profiles in a mouse model of diet-induced obesity. Front. Pharmacol. 10, 842.

Zhang, P., Zhu, W., Wang, D., Yan, J., Wang, Y., Zhou, Z., He, L., 2017. A combined NMR- and HPLC-MS/MS-based metabolomics to evaluate the metabolic perturbations and subacute toxic effects of endosulfan on mice. Environ. Sci. Pollut. Res. Int. 24, 18870–18880.

Zhao, Q., Yang, R., Liu, F., Wang, J., Hu, D.-D., Yang, X.-W., Li, F., 2017. Metabolomics reveals that PPARα activation protects against lithocholic acid-induced liver injury. RSC Adv. 7, 49849–49857.

Zhao, W., Zitzow, J.D., Ehresman, D.J., Chang, S.-C., Butenhoff, J.L., Forster, J., Hagenbuch, B., 2015. Na+/taurocholate cotransporting polypeptide and apical sodium-dependent bile acid transporter are involved in the disposition of perfluoroalkyl sulfonates in humans and rats. Toxicol. Sci. 146, 363–373.